Available online at www.sciencedirect.com
SCIENCE DIRECT
ELSEVIER
Renewable Energy 31 (2006) 517–535
RENEWABLE ENERGY
www.elsevier.com/locate/renene

Numerical simulation of the airflow and temperature distribution in a lean-to greenhouse

Wei Chen[a,*], Wei Liu[b]

[a]*College of Merchant Marine, Shanghai Maritime University, Shanghai 200135, People's Republic of China*
[b]*School of Energy and Power Engineering, Huazhong University of Science and Technology, Wuhan, Hubei 430074, People's Republic of China*

Received 16 April 2004; accepted 18 April 2005
Available online 10 August 2005

Abstract

In this paper, heat transfer and flow in a lean-to passive solar greenhouse has been studied. A mathematical model based on energy equilibrium and a one-dimensional mathematical model for the unsaturated porous medium have been founded and developed to predict the temperature and moisture content in soil and the enclosed air temperature in the greenhouse. On the condition that plant and massive wall is neglected, the air is mainly heated by the soil surface in the greenhouse, which absorbs the incident solar radiation. With increase in depth, the variation of the temperature and moisture content in soil decreases on account of ambient, and the appearance of the peak temperature in soil postpone. Solar radiation absorber, heat storage and insulation are the main effects of the north massive wall on greenhouse, which is influenced by the structure and the material. The specific heat capacity and thermal conductivity of wall material have a remarkable effect on the north wall temperature. The build-up north wall with thermal insulation material may be chosen for greenhouse. The temperature distribution and gas flow in greenhouse is influenced by the cover material of the inside surface of the north wall and the inclined angle of greenhouse roof. All results should be taken into account for a better design and run of a greenhouse.

Keywords: Greenhouse; Heat transfer; Soil; Wall

* Corresponding author. Tel.: +86 21 58855200x2119; fax: +86 21 68620259.
E-mail address: weichen96@sina.com (W. Chen).

0960-1481/$ - see front matter © 2005 Elsevier Ltd. All rights reserved.
doi:10.1016/j.renene.2005.04.015

Nomenclature

A	area (m^2)
c	specific heat (J/kg K)
c_1	constant for the turbulence model
c_2	constant for the turbulence model
c_μ	constant for the turbulence model
D_l	diffusivity of water in porous medium (m^2/s)
f_1	turbulence model coefficient
f_2	turbulence model coefficient
f_μ	turbulence model coefficient
g	gravitational acceleration vector (m/s^2)
G	turbulence model coefficient
G_{ssun}	rate of solar flux absorbed by soil surface in the greenhouse (W/m^2)
G_{wsun}	rate of solar flux absorbed by the north wall inside the greenhouse ($W/m^{2)}$
G_{gsun}	rate of solar flux absorbed by the glass enclosure of the greenhouse (W/m^2)
h_m	convective mass transfer coefficient (m/s)
k	turbulence kinetic energy
k_l	liquid water thermal conductivity (W/(m K))
k_{lw}	unsaturated permeability of liquid water (m^2)
k_{gw}	equivalent permeability of gas-mixture (m^2)
k_m	apparent thermal conductivity (W/(m K))
k_s	solid thermal conductivity (W/(m K))
k_g	gaseous thermal conductivity (W/(m K))
k_w	thermal conductivity for surface of the north wall absorber (W/(m K))
K_g	hydraulic conductivity of gas (m/s)
K_l	hydraulic conductivity of liquid (m/s)
$\dot{m}$	mass rate of phase change ($kg/(m^3\ s)$)
p	pressure (Pa)
Pr	Prandtl number
Q_{as}	convective heat exchange between the air and the surface of soil in greenhouse (J)
Q_{aw}	convective heat exchange between the air of the greenhouse and the inside surface of the north wall (J)
Q_{awo}	convective heat exchange between the ambient and the outside surface of the north wall (J)
Q_{cai}	convective heat exchange between the air of the greenhouse and the glass enclosure of greenhouse (J)
Q_{cao}	convective heat exchange between the ambient and the glass enclosure of greenhouse (J)
Q_{rg}	thermal radiation exchange of the glass enclosure with the soil surface and the north wall surface in the greenhouse (J)
Q_{rs}	thermal radiation exchange of the soil surface with the glass enclosure and the north wall surface in the greenhouse (J)

Q_{rw} thermal radiation exchange of the inside surface of the north wall with he soil surface and the glass enclosure in the greenhouse (J)
Q_{sky} thermal radiation exchange between the glass enclosure of greenhouse and sky (J)
Q_{skyw} thermal radiation exchange between the outside surface of the north wall and sky (J)
r latent heat (J/kg)
Re Reynolds number
S source term
T temperature (K(°C))
T_{ao} ambient temperature (°C)
u velocity component in x-direction (m/s)
v velocity component in y-direction (m/s)
x horizontal coordinate (m)
y vertical coordinate (m)

Greek symbols
β thermal expansion coefficient ($1/K$)
τ time (s)
Γ exchange coefficient
ε dissipation rate of turbulent kinetic
σ_ε constant for the turbulence model
σ_k constant for the turbulence model
σ_t constant for the turbulence model
μ dynamic viscosity (kg/(m s))
μ_{eff} effective dynamic viscosity for the turbulence model (kg/(m s))
ν kinematic viscosity (m^2/s)
ρ density (kg/m^3)
ρ^o density of saturated water (kg/m^3)
ϕ dependent variable
θ phase content
θ_{ls} moisture content of the soil surface

Subscripts
c cold wall
g gaseous
l liquid water
m apparent mean
s solid, soil
t turbulent
w north wall

Superscripts
- average

1. Introduction

Passive solar greenhouses are often used to grow plants of high quality in cold climates. Soil temperature, air temperature and airflow distribution are interactive in a greenhouse and affect plant growth and development. The energy balance has been estimated and the air temperature have been measured and predicted in greenhouse under various conditions by Sharma et al. [1], Gabriel et al. [2], Kurklu and Bilgin [3]. A lean-to greenhouse in which the incident solar radiation can be fully absorbed has been widely, was reported by Xing et al. [4], Jorge R. Barral et al. [5]. During the period that the seed exists in soil or the plant is small, and the ground is mainly bare soil in greenhouse, plants can be neglected and the ground of greenhouse may be assumed as bare soil. As a kind of unsaturated porous media, soil consists of soil particles, liquid water, gaseous mixture of vapor and air and other chemical and biological substances. Some typical theories of heat and mass transfer in porous media were established by Philip and DeVries [6], Luikov [7], Slattery [8], Whitker [9] and research in the soil area have been reported by Milly [10]. However, the effects between the temperature of soil surface and the air temperature in greenhouse are also significant and some theoretical aspects of moisture movement in porous materials need to be improved.

A north thermal storage costs little and is used in greenhouse as reported in Santamouris et al. [11]. A north storage wall consisting of 60 cm wide concrete blocks was utilized in 30 small size greenhouses. The temperature of the air inside the greenhouse was 15–20 °C higher than the minimum ambient temperature which was reported by Santamouris et al. [12]. The north wall can also be constructed with stones in a 350 m^2 greenhouse. This system maintained inside temperature 1–2 °C higher than the minimum outdoor air temperature reported by Sallanbas [13]. Thus, the north wall has a great influence on the temperature in greenhouse.

In the present work, a lean-to greenhouse, shown schematically in Fig. 1, has been investigated. A mathematical model based on energy equilibrium and a one-dimensional mathematical model for the unsaturated porous media has been formulated. The thermal performance of the north heat storage wall in the greenhouse, influenced by heat-insulation and material of the wall, has been studied. The effects of the cover material of the north wall inside surface on the temperature distribution and gas-flow in the greenhouse have

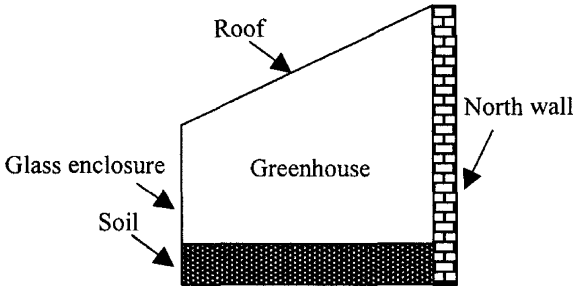

Fig. 1. Schematic of a lean-to type passive solar.

also been investigated. The present study focuses on selecting efficient strategies for a better design and running of a greenhouse.

2. System description and mathematical analysis

2.1. System description

A lean-to passive solar greenhouse with a south inclining roof under investigation is shown schematically in Fig. 1. The roof and wall except the north wall consists of plate glass. A 60 cm wide massive wall is built at the north side of the greenhouse, which has two functions, one as a solar absorber, the other as a heat storage and insulator. The ground of greenhouse is assumed as bare soil.

2.2. Theoretical modeling

In discussing the physical mechanisms of heat and mass transfer in the soil by the conservational differential equations, some basic assumptions are made as follows:

Soil is regarded as homogeneous and isotropic medium with no distension or contraction;
Subject to local thermal equilibrium throughout the analysis domain of soil;
Liquid phase and gas phase in funicular remain continuous states, respectively in soil;
Boussinesq's approximation is used to account for the gaseous density variation in soil;
Ideal-gas treatment for gaseous mixture in pore space of porous matrix;

As the viscosity dissipation effects and the accelerated pressure drop of the liquid water are neglected, the liquid water in soil is drawn by gravitation and capillary attraction caused by moisture content gradient of the soil. As the viscosity dissipation effects of gas are neglected, the gas in soil is drawn by buoyancy, Darcy's resistance and pressure drop of gas flow, and the three kinds of above force, buoyancy, Darcy's resistance and pressure drop of gas flow, keep equilibrium in soil. Therefore, a one-dimensional mathematical model for the unsaturated porous soil has been founded by Zhang and Liu [14].

Continuity equations:For water liquid:

$$\frac{\partial \rho_l \theta_l}{\tau} + \frac{\partial \rho_l \theta_l u_l}{y} = -\dot{m} \tag{1}$$

For gas:

$$\frac{\partial \rho_g \theta_g}{\tau} + \frac{\partial \rho_g \theta_g u_g}{y} = \dot{m} \tag{2}$$

$$\theta_l + \theta_g + \theta_s = 1 \tag{3}$$

Momentum equations:For water liquid:

$$u_{\mathrm{l}} = -\frac{D_{\mathrm{l}}}{\theta_{\mathrm{l}}}\frac{\mathrm{d}\theta_{\mathrm{l}}}{\mathrm{d}y} - \frac{K_{\mathrm{l}}}{\theta_{\mathrm{l}}} \tag{4}$$

For gas:

$$u_{\mathrm{g}} = \frac{K_{\mathrm{g}}\beta(T_{\mathrm{s}} - T_{\mathrm{c}})}{\theta_{\mathrm{g}}} + \frac{\mathrm{d}p}{\mathrm{d}y}\frac{K_{\mathrm{g}}}{\rho_{\mathrm{g}}\theta_{\mathrm{g}}g} + \frac{\theta_{\mathrm{l}}}{\theta_{\mathrm{g}}}u_{\mathrm{l}} \tag{5}$$

Energy equation

$$(cp)_{\mathrm{m}}\frac{\mathrm{d}T_{\mathrm{s}}}{\mathrm{d}t} + (\theta_{\mathrm{l}}\rho_{\mathrm{l}}c_{\mathrm{l}}u_{\mathrm{l}} + \theta_{\mathrm{g}}\rho_{\mathrm{g}}c_{\mathrm{g}}u_{\mathrm{g}})\frac{\mathrm{d}T_{\mathrm{s}}}{\mathrm{d}y} = \frac{\mathrm{d}}{\mathrm{d}y}\left(k_{\mathrm{m}}\frac{\mathrm{d}T_{\mathrm{s}}}{\mathrm{d}y}\right) - r\dot{m} \tag{6}$$

The apparent physical properties of unsaturated porous soil are simply set to the mean ones, say:

$$(cp)_{\mathrm{m}} = \theta_{\mathrm{l}}\rho_{\mathrm{l}}c_{\mathrm{l}} + \theta_{\mathrm{g}}\rho_{\mathrm{g}}c_{\mathrm{g}} + \theta_{\mathrm{s}}\rho_{\mathrm{s}}c_{\mathrm{s}}, \qquad k_{\mathrm{m}} = \theta_{\mathrm{l}}k_{\mathrm{l}} + \theta_{\mathrm{g}}k_{\mathrm{g}} + \theta_{\mathrm{s}}k_{\mathrm{s}},$$

The hydraulic conductivity K_{l}, K_v was defined from the previous work by Liu and Peng [15], $K_l = k_{\mathrm{lw}}g/v_{\mathrm{l}}$ $K_{\mathrm{g}} = k_{\mathrm{gw}}g/v_{\mathrm{g}}$

Above the soil in the greenhouse, the airflow is considered as turbulent natural convection and the Low-*Re*-*k*-ε model of turbulence is used, which is an extension of the high-*Re*-*k*-ε model that can reproduce the wall damping of turbulence and hence can be used across the viscous sub-layer. The equations for continuity, velocity components and temperature take the form which was given by Iacovides and Raisee [16]:Continuity equation:

$$\frac{\partial(\rho u)}{\partial x} + \frac{\partial(\rho v)}{\partial y} = 0 \tag{7}$$

Momentum equations

$$\frac{\partial(\rho u)}{\partial \tau} + \frac{\partial(\rho u u)}{\partial x} + \frac{\partial(\rho v u)}{\partial y} = \frac{\partial}{\partial x}\left(\mu_{\mathrm{eff}}\frac{\partial u}{\partial x}\right) + \frac{\partial}{\partial y}\left(\mu_{\mathrm{eff}}\frac{\partial u}{\partial y}\right) + S_u \tag{8}$$

$$\frac{\partial(\rho v)}{\partial \tau} + \frac{\partial(\rho u v)}{\partial x} + \frac{\partial(\rho v v)}{\partial y} = \frac{\partial}{\partial x}\left(\mu_{\mathrm{eff}}\frac{\partial v}{\partial x}\right) + \frac{\partial}{\partial y}\left(\mu_{\mathrm{eff}}\frac{\partial v}{\partial y}\right) + S_v \tag{9}$$

The source terms in momentum equation are:

$$S_u = -\frac{\partial p}{\partial x} + \frac{\partial}{\partial x}\left(\mu_{\mathrm{eff}}\frac{\partial u}{\partial x}\right) + \frac{\partial}{\partial y}\left(\mu_{\mathrm{eff}}\frac{\partial v}{\partial x}\right) \tag{10}$$

$$S_v = -\frac{\partial p}{\partial y} + \frac{\partial}{\partial x}\left(\mu_{\mathrm{eff}}\frac{\partial u}{\partial y}\right) + \frac{\partial}{\partial y}\left(\mu_{\mathrm{eff}}\frac{\partial v}{\partial y}\right) + \rho g\beta(T - T_{\mathrm{C}}) \tag{11}$$

General transported fluid scalar, ϕ (e.g. T, k, ε)

$$\frac{\partial(\rho\phi)}{\partial\tau}+\frac{\partial(\rho u\phi)}{\partial x}+\frac{\partial(\rho v\phi)}{\partial y}=\frac{\partial}{\partial x}\left(\Gamma_\phi\frac{\partial\phi}{\partial x}\right)+\frac{\partial}{\partial y}\left(\Gamma_\phi\frac{\partial\phi}{\partial y}\right)+S_\phi \tag{12}$$

Where Γ_ϕ is the exchange coefficient for the transport of property ϕ which is for T, k and ε:

$$\Gamma_T=\frac{\mu}{\mathrm{Pr}}+\frac{\mu_\mathrm{t}}{\sigma_\mathrm{t}};\qquad \Gamma_k=\mu+\frac{\mu_\mathrm{t}}{\sigma_k};\qquad \Gamma_\varepsilon=\mu+\frac{\mu_t}{\sigma_k}.$$

The source terms in the ϕ equations are:

$$S_k=\mu_\mathrm{t}G-\rho\varepsilon-2\mu\left(\frac{\partial k^{1/2}}{\partial y}\right)^2 \tag{13}$$

$$S_\varepsilon=\frac{\varepsilon}{k}c_1f_1\mu_\mathrm{t}G-c_2\rho\frac{\varepsilon^2}{k}f_2+2\frac{\mu\mu_\mathrm{t}}{\rho}\left(\frac{\partial^2u}{\partial y^2}\right)^2 \tag{14}$$

$$S_T=0,$$

$$G=\frac{\mu_\mathrm{t}}{\rho}\left\{2\left[\left(\frac{\partial u}{\partial x}\right)^2+\left(\frac{\partial v}{\partial y}\right)^2\right]+\left(\frac{\partial u}{\partial y}+\frac{\partial v}{\partial x}\right)^2\right\}$$

The expression for the turbulent viscosity (15), now includes the damping function f_μ, given by Eq. (16), in which the damping parameter R_t is the local Reynolds number of turbulence defined as $R_\mathrm{t}=\rho k^2/(\mu\varepsilon)$:

$$\mu_\mathrm{t}=\rho c_\mu f_\mu k^2/\varepsilon \tag{15}$$

$$f_\mu=\exp[-3.4/(1+0.02R_\mathrm{t})^2] \tag{16}$$

The damping function f_1, f_2 for the generation rate of ε is determined with respect to decaying, grid-generated turbulence:

$$f_2=1-0.3\exp(-\mathrm{Re}_\mathrm{t}^2) \tag{17}$$

$$f_1=1$$

The turbulence model contains five constants, which were assigned the following values

$$c_\mu=0.09,\qquad c_1=1.44,\qquad c_2=1.92,\qquad \sigma_k=1,\qquad \sigma_\varepsilon=1.3,\qquad \sigma_t=1$$

The heat transfer through the north massive wall of the greenhouse is governed by heat conduction equation:

$$\frac{\partial T}{\partial\tau}=\frac{k_\mathrm{w}}{\rho_\mathrm{w}c_\mathrm{w}}\left(\frac{\partial^2T}{\partial x^2}+\frac{\partial^2T}{\partial y^2}\right) \tag{18}$$

2.3. Boundary conditions and initial conditions

Numerical simulations were performed under the ambient and operative conditions. A typical cold and sunny of November day in Wuhan, China was considered, and the outdoor temperature [17] and the solar radiative variation [18] were given by Eqs. (19) and (20).

$$T_{ao}(\tau) = \overline{T_{ao}} + T_{ar}\cos\left(\frac{\pi}{12}(\tau - 14)\right) \tag{19}$$

$$G_{sun}(\tau) = \hat{G}_{sun}\sin\left(\frac{\tau - a}{b - a}\pi\right), \quad a < \tau < b \tag{20}$$

Where $\overline{T_{ao}}$ is for average outside temperature of 10 °C; T_{ar} for amplitude temperature of 5 °C; $\hat{G}_{sun}$ for maximum solar radiation of 350 W/m^2; a for sunrise hour at 6:00 in the morning; b for sunset hour at 18:00 in the afternoon; τ for time hours.

The energy equilibrium equations for different components of the proposed passive solar greenhouse have been written with the following assumptions:

There was no stratification in the air temperature of the greenhouse.
No temperature gradient exists along the glass enclosure surface of greenhouse, on the surface of the soil and on the north wall surface inside the greenhouse.
The surface of the soil, enclosure and covers in greenhouse are considered as gray body.
The air radiation absorbency in the greenhouse is neglected.

The initial and boundary conditions from the energy balance equations are given below.For the glass enclosure and roof of the greenhouse

$$G_{gsun} + Q_{sky} + Q_{cai} + Q_{cao} + Q_{rg} = 0 \tag{21}$$

$$T = T_{gb}, \qquad u = 0, \qquad v = 0$$

For the inside surface of the north wall

$$A_w k_w \frac{dT_w}{dx} = G_{wsun}A_w + Q_{aw} + Q_{rw} \tag{22}$$

$$u = 0, \qquad v = 0$$

For the outside surface of the north wall

$$A_w k_w \frac{dT_w}{dx} = Q_{awo} + Q_{skyw} \tag{23}$$

For the soil surface in the greenhouse

$$A_s k_m \frac{dT_s}{dy} = G_{ssun}A_s + Q_{rs} + Q_{as} \tag{24}$$

$$u = 0, \quad v = 0$$

Moisture content,

$$\dot{m} = A_s h_m(\theta_{ls}\rho_s^o - \theta_a\rho_a^o), (\theta_l\rho_l u_l + \theta_g\rho_g u_g) = \dot{m} \tag{25}$$

At depth of 1 m in the soil: T=constant; Moisture content,

$$\frac{\partial\theta_l}{\partial y} = 0 \tag{26}$$

Initial conditions $\tau = 0$, $T = constant$, $\theta_l = \theta_l(y)$, $\theta_s = constant$

3. Numerical procedure

To investigate the interactive effects between the soil temperature and air temperature in the greenhouse, and the temperature and moisture content in the soil, the north wall and the plane is neglected, the Eqs. (1)–(6) together with the boundary conditions, Eqs. (24)–(26), were solved by a finite difference method. The time step was of much concern and several values of $\Delta\tau$ were examined for the grid chosen. It had been found that the maximum deviation between the results using $\Delta\tau = 10$ s and $\Delta\tau = 20$ s was only 1.5%. Hence, the time steps of $\Delta\tau = 20$ s together with the grid size of 80 for the depth of the soil were used for the unsteady-state numerical calculations performed in this study.

To study the effect of the north wall inside surface on the temperature and airflow in the greenhouse, the governing Eqs. (7)–(17) together with the boundary conditions, Eqs. (21), (22) and (24), were solved with the SIMPLER method by Patankar [19]. The computer code based on the mathematical formulation discussed earlier and the SIMPLER method is validated for various cases publish in the literature reported by Tao [20]. The control-volume formulation utilized in this method ensures continuity of the convective and diffusive fluxes as well as overall momentum and energy conservation. To test the grid independence, two different grid sizes, 108×128 and 128×158 had been employed, but its influence on the calculating results is small. Therefore, a grid of 108×128 had been chosen.

At the outdoor temperature of 10 °C and the solar radiant intensity of 350 W/m^2, steady-state solutions were attempted to draw the isothermals and streamlines of the greenhouse.

To analyze the influence of the north wall on the air temperature in greenhouse and its thermal behavior, the effect of the plant and ground is neglected, the SIMPLER method were also used to solve the Eqs. (7)–(18) together with the boundary conditions, Eqs. (21)–(23). This method allows the numerical treatment of the pure heat conduction in the north wall by introducing an artificial viscosity (10^{30}), which ensures that a zero velocity prevails throughout this region.

In order to ensure the convergence of calculating procedure, some technical treatments such as relaxation and error feedback, were adopted. The accuracy of the computations was checked using energy conservation within the system set at 0.1%.

To analyze the effect of materials and structure on the heat transfer of the wall, rock, concrete, soil-brick and slag-wool given by Ma [21] were chosen with:

Rock: $\rho = 1400$ kg/m^3, $c = 0.836$ kJ/(kg K), $k_s = 1.54$ W/(m K)
Concrete: $\rho = 2400$ kg/m^3, $c = 0.836$ kJ/(kg K), $k_s = 1.53$ W/(m K)
Soil-brick: $\rho = 2000$ kg/m^3, $c = 0.878$ kJ/(kg K), $k_s = 0.79$ W/(m K)
Slag-wool: $\rho = 350$ kg/m^3, $c = 0.753$ kJ/(kg K), $k_s = 0.06$ W/(m K)

4. Experiments

Measurement of the temperatures were made with thermocouples connected with numerical voltage setting, which were placed on the soil surface and at the depth of 8, 15 cm within soil, in the middle of the greenhouse. The ambient temperatures were measured with mercury thermometer. The measurement of the airflow speed was conducted with an anemometer. Solar radiation was measured with an actinography. The type of MP-406 Moisture probes (made in ICT corporation in Australia) were placed at the depth of 4, 16 cm within sand soil. The type of CYH-3605A humidity instrument was placed in the air space of the greenhouse.

5. Results and discussion

5.1. The performance of the air temperature and soil temperature in the greenhouse

From Fig. 2a, we can find that due to the variation of solar irradiation, the temperature difference among the ambient, the soil surface and air in the greenhouse changes. At 14:00 in the afternoon, there was a difference of more than 15 °C between the temperature of the soil surface and the ambient temperature, and the air of the greenhouse was also 10 °C higher than the outdoor. In contrast, while no solar radiation was available and no heat-insulated method was taken for the glass enclosure, the temperature in the greenhouse drops quickly, the soil surface temperature is slightly higher than the air temperature in the greenhouse and there is a slight of temperature difference between the air of the greenhouse and the ambient temperature. The soil surface temperature is above the air temperature all the time. Thus, the incident solar radiation absorbed by the soil surface has been divided into two parts, one heat the air in the greenhouse, the other transfers into the inside of soil.

As shown in Fig. 2b and c, with increase in depth, the variation range of temperature reduces and the peak temperature of the soil moves to the inside, and the appearance of that postpones, accordingly, the influence of environment on soil temperature decreases. At a certain depth, for instance, at 0.8–1 m, the soil temperature remains constant. When there is no solar irradiation available, the heat stored in the soil bed transfers to the surface and is released to outside of the soil. So, there is thermal inertia in soil bed. The predicted values of temperature are corresponding to the measures, as shown in Fig. 3.

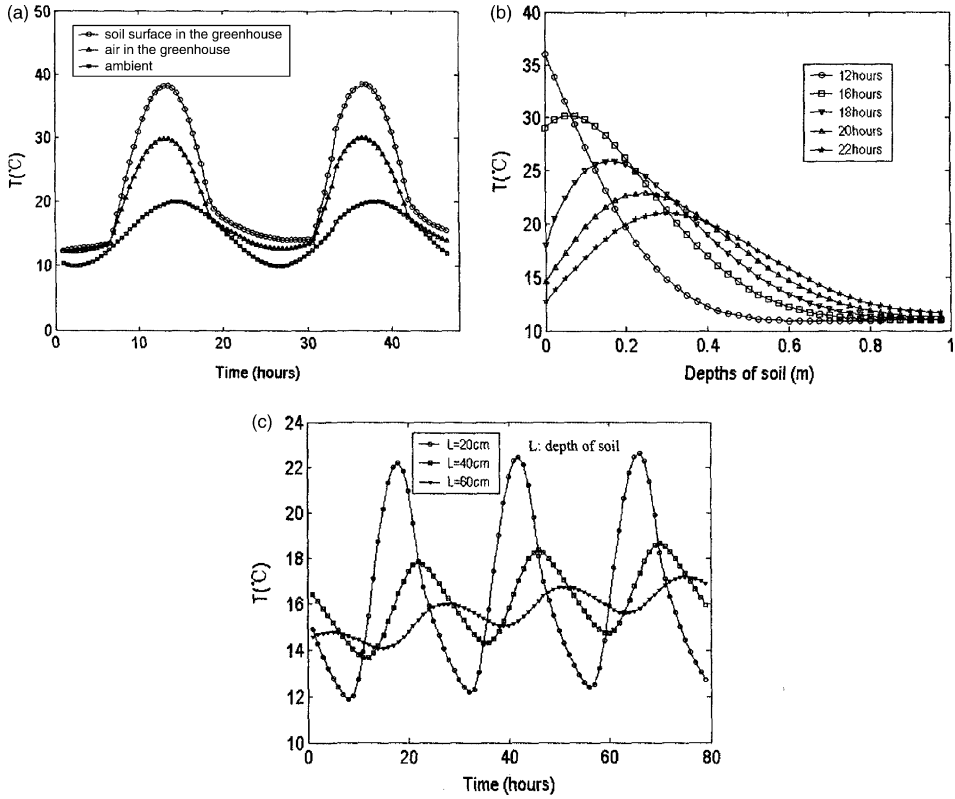

Fig. 2. Predicted temperature of soil and air in greenhouse (a) Comparison of temperature among ambient, soil surface and air in greenhouse (b) temperature distribution in soil in a day (c) Hourly values of temperature at 20, 40, and 60 cm in soil.

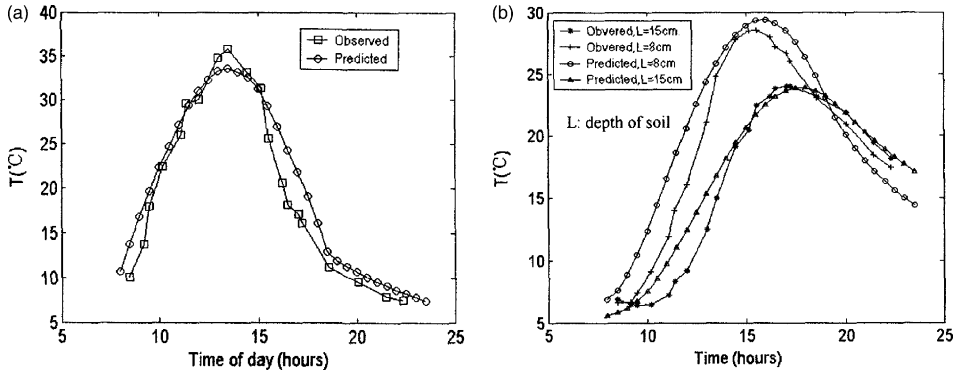

Fig. 3. Comparison between measured and predicted values of temperature in greenhouse (a) air temperature (b) at 8 and 15 cm in soil.

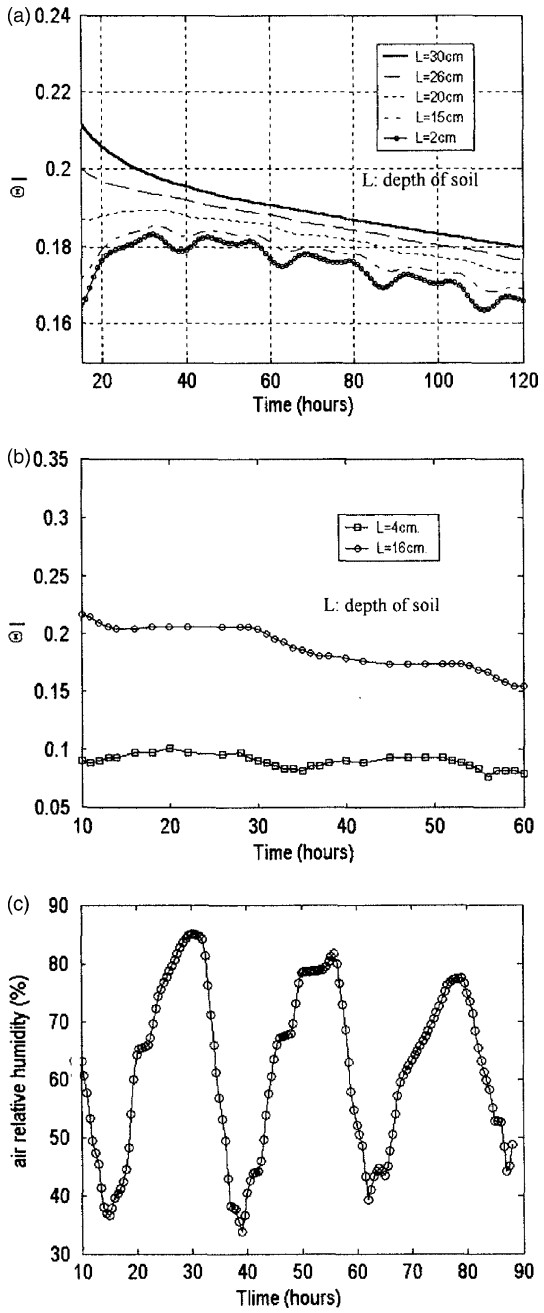

Fig. 4. Hourly values of moisture content in greenhouse (a) predicted values at 2, 15, 20, 25 and 30 cm in soil (b) measured values at 4, 16 cm in soil (c) measured values of air relative humidity in greenhouse.

5.2. The performance of moisture content in the soil

From Fig. 4a–c, it can be seen that due to the periodic variation of the solar radiation, the temperature and relative humidity of ambient, the moisture content of the soil bed upside changes regularly, which was vaporized more in the daytime than in the night time. As the amount of water from the bottom of the soil bed was less than that of water lost to the air space in the daytime, the moisture content in the upside of soil bed decreased greatly, In contrast, owing to the reduction of the air temperature, the increase of the air relative humidity and no solar irradiation in the night, the water from the bottom of the soil bed was more than the water vaporized, and so the moisture content in the upside of the soil bed increased. Without irrigation, the moisture content in soil declines. The wavy variation of the moisture content disappeared and the effects of the outside on the moisture content were reduced with increase in depth of the soil. The predicated moisture content profile in soil was corresponding to the observed one in experiment field plots.

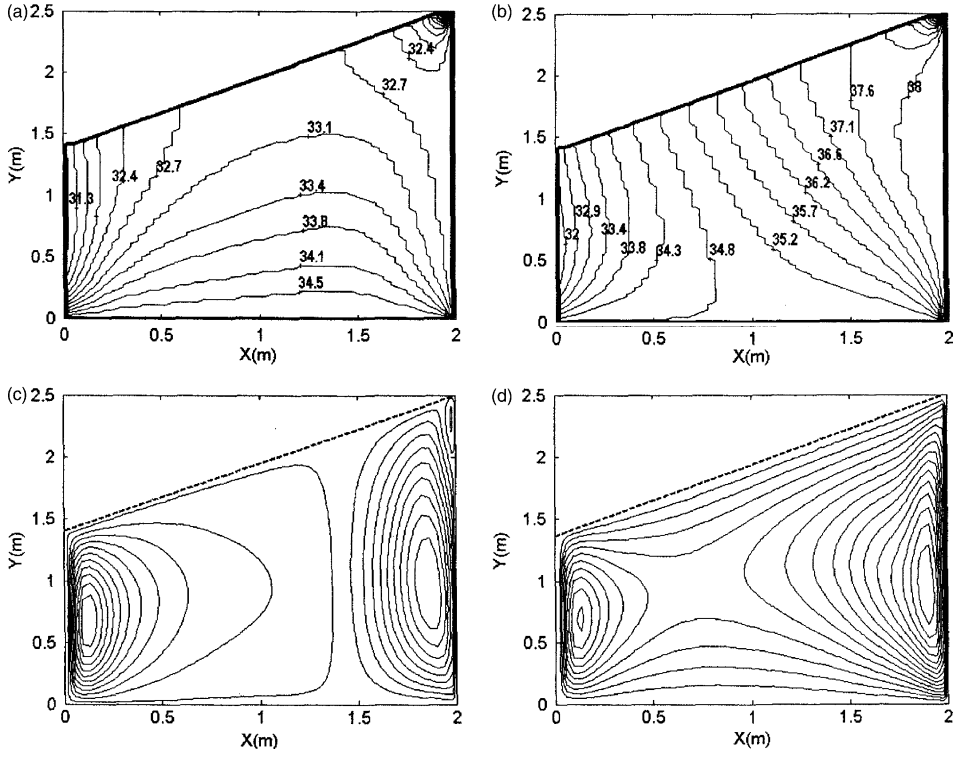

Fig. 5. Airflow and temperature fields for different cover materials of the north wall inside surface above soil in greenhouse (a) isotherms (°C) for a concrete layer on the north wall inside surface (b) isotherms (°C) for blacked layer on the north wall inside surface (c) streamlines for a concrete layer on the north wall inside surface (d) streamlines for a blacked layer on the north wall inside surface.

5.3. Effect of the north-wall inside surface covered with different material

From Fig. 5, we find that the temperature of the soil surface and the inside surface of the north wall are higher comparatively, which are the main solar absorber in the greenhouse. Due to the heat exchange between the glass enclosures and ambient, the air temperature near the glass enclosure is lower in the greenhouse. The further position from the soil surface and the north wall surface in greenhouse is, the lower temperature of the air in greenhouse is. Affected by the temperature distribution in the heating system, the two non-symmetrical air cycles have been produced in the greenhouse.

Comparison between Fig. 5a and c and Fig. 5b and d shows that by contrast with concrete cover, the solar radian absorptance of the inside surface of the north wall, which is covered with black paint, increases and is above that of the soil surface. Thus, the effect of the north wall inside surface on the temperature distribution and gas-flow in the greenhouse increases and the average air temperature of the greenhouse go up. In addition, to increase the irradiation intensity of light in the greenhouse, the inside surface of the north wall may be covered with white paint, and so the solar radian reflectivity of the north wall rises. Therefore, solar irradiation can be used to meet the requirement of the temperature or light irradiation in the greenhouse by changing the cover material of the inside surface of the north wall.

5.4. Effect of the greenhouse roof inclination

From comparison made between Fig. 5 and Fig. 6, it can be seen that as the solar radian absorptance of the soil surface is above that of the north wall surface inside the greenhouse and the north wall keeps a certain height, the inclined angle of greenhouse roof has great effects on temperature distribution and gas flow in the greenhouse. With increase in the greenhouse roof inclination, the average air temperature of the greenhouse rises, the influences of the north wall surface on the airflow within the greenhouse increase and the air cycles change greatly.

5.5. Thermal performance for the north massive wall of difference structure and material

Observing Fig. 7, we can find that during the heating period, the inside surface of the north wall has comparatively higher temperature, thus the solar radiation absorbed by the north wall is utilized to raise the air temperature and the thermal storage wall temperature. When solar radiation is not available, as the heat has already been stored in the massive thermal storage wall, the inside of this wall with relatively higher temperature can transfer to the surface and still heat the air in the greenhouse.

From comparison between Fig. 8a and b, it can be seen that with decrease in intensity of solar irradiation, the peak temperature of the wall reduces and moves to the inside, and the appearance of the peak temperature postpones. There is no effect of solar irradiation on the outside of the north wall, so the variation range of the north outside surface is less comparatively. Owing to the heat storage in the wall, the temperature near the outside surface of the wall at 18:00 in the afternoon is higher than that at 10:00 and 8:00 in the morning. On the condition that the temperature of the inside and outside surface nearly

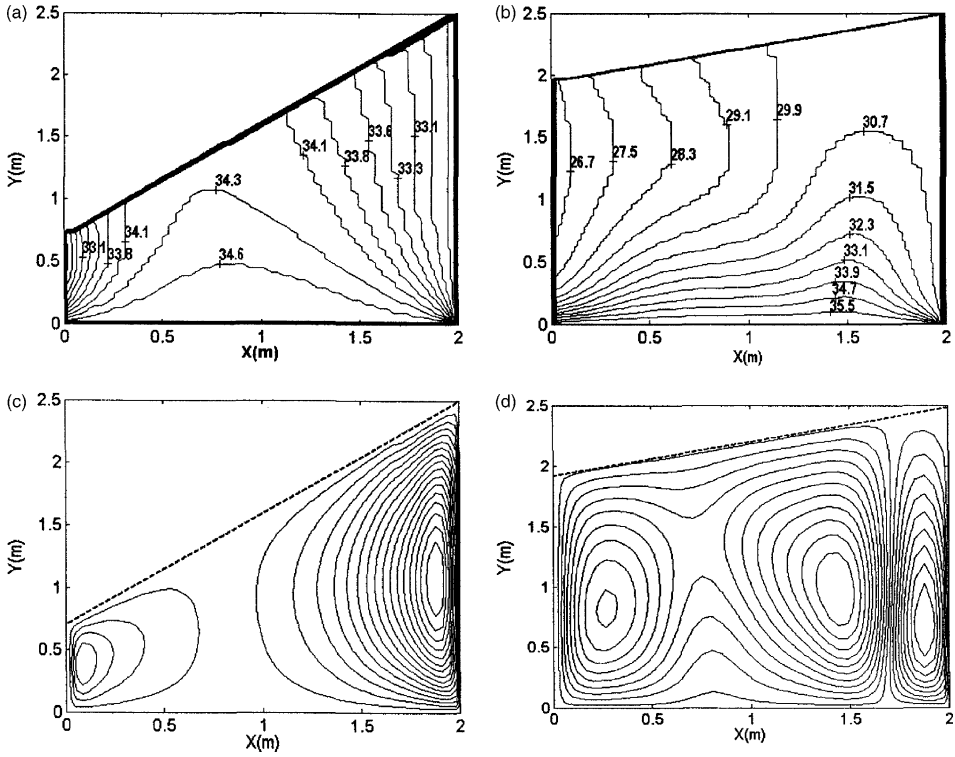

Fig. 6. Airflow and temperature fields for different south inclination of the roof in greenhouse with a concrete layer on the inside surface of the north wall (a) isotherms (°C) for a 45° south inclination of the roof (b) isotherms (°C) for a 15° south inclination of the roof (c) streamlines for a 45° south inclination of the roof (d) streamlines for a 15° south inclination of the roof.

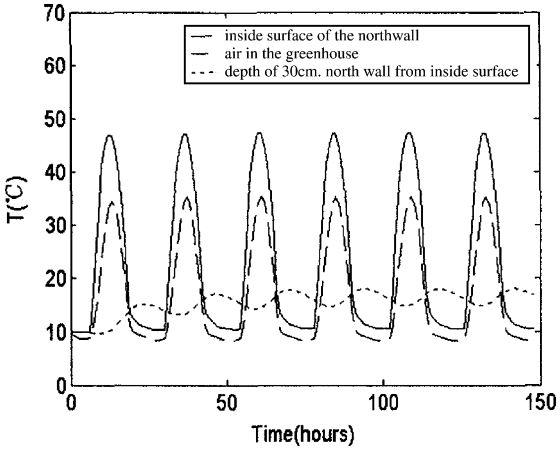

Fig. 7. Comparison predicted values of temperature among on inside surface and at 30 cm in the north wall, air in greenhouse.

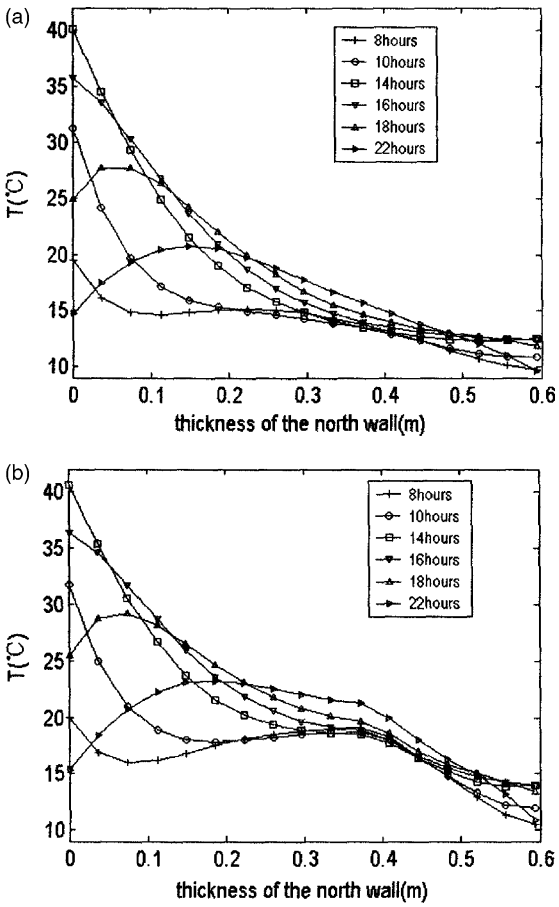

Fig. 8. Predicted values of temperature distribution in the north wall in a day (a) the north wall of 60 cm wide concrete (b) the north build-up wall of 40 cm wide concrete and 20 cm wide slag-wool.

equals, the temperatures of the build-up wall on the side of the concrete and the temperature difference between the both sides of the slag-wool of the build-up wall are obviously higher than that of the concrete wall on the same region. Therefore, the heat loss of the build-up wall is less and the average temperature is higher in comparison to the concrete, shown in Fig. 9. Due to more heat stored in the build-up wall on the side of the concrete, the temperature decreases from the inside surface and the interface of the slag-wool and the concrete to the inside of the build-up wall at 8:00 and 10:00 in the morning.

Fig. 10 shows that the temperatures of different wall materials change versus time for rock, concrete and soil-brick, which have the typical characteristics for thermal storage. With increase in the thickness of the north wall from the inside, the wavy variation of the temperature decreases. The appearance of the peak wall temperature at the same thickness postpones with increase in the specific heat capacity (ρc) and decrease in the thermal conductivity of the wall material.

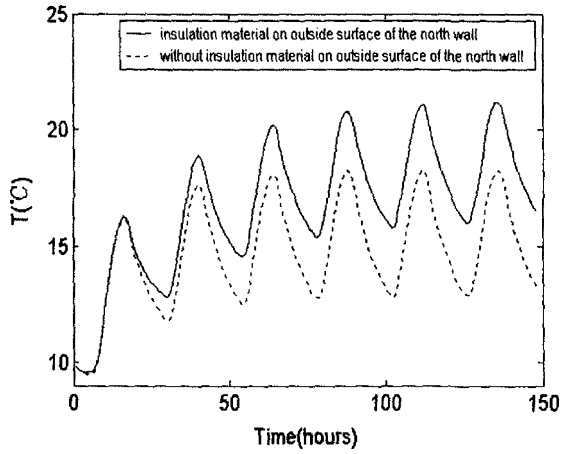

Fig. 9. Comparison of predicted mean temperature between build-up north wall of 40 cm wide concrete and 20 cm wide slag-wool and the north wall of 60 cm concrete.

It is clear that during the period that solar radiation is available, the temperature of wall increases when the material (rock) with higher thermal conductivity is used and the temperature of wall decreases greatly with increase in the specific heat capacity (ρc). However, when the sun is not shining, the temperature of wall with higher (ρc) value is slightly higher than that with lower (ρc) value. Therefore, thermal conductivity and specific heat capacity (ρc) of the wall material play an important role in the heat storage of the north wall.

When designing or building the north thermal storage wall for greenhouse, the build-up wall, which is composed of the insulation layer and the heat storage layer with relatively higher conduction and specific heat capacity (ρc), will be chosen. As a result, when there is solar radiation available, the temperature of wall is higher comparatively and more heat

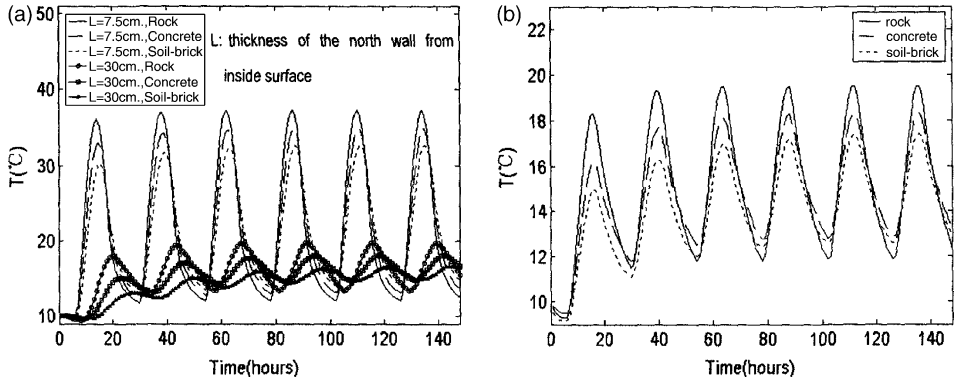

Fig. 10. Hourly values of temperature for the north wall of different material (a) at 7.5, 15 cm in the north wall from wall inside surface (b) average temperature of the north wall.

can be stored and heat loss decreases. In contrast, at night or in a cloudy day, more heat of the wall releases to the greenhouse.

6. Conclusion

From the above discussion, we can conclude that the temperature of the air, the soil and the wall in greenhouse is mainly influenced by solar radiation. With increase in depth, the periodic variation range of the soil temperature and the moisture content in soil decreases, and the appearance of the peak temperature of soil are delayed. Heat absorption, storage and insulation are the main function of the north wall in greenhouse. The cover material of the inside surface of the north wall, which is black paint or white paint, could be selected to increase the absorption or reflection of solar radiation to meet the requirement of the temperature or the light radiation in greenhouse. With increase in inclination of the greenhouse roof, the mean temperature of air increases comparatively and the airflow in the greenhouse improves. The build-up wall, which consists of two layers, may be utilized in greenhouse, the outside works as insulation, and the inside is heat storage, so the heat loss decreases. The specific heat capacity (ρc) and thermal conductivity of the heat storage layer increase, as a result, more heat could be stored in the north wall and supplied to the greenhouse.

Acknowledgements

National Natural Science Foundation of China and Doctoral Foundation of Education Ministry of China.

References

[1] Sharma PK, Tiwari GN, Sorayan VPS. Parametric studies of a greenhouse for summer conditions. Energy 1996;23(9):733–44.
[2] Pita Gabriel PA, Pontes Manuel, Vargues Alberto. Mediterranean greenhouse energy balance. Acta Horticulture 1998;456:375–82.
[3] Kurklu Ahmet, Bilgin Sefai. A study on the solar energy storing rock-bed to heat a polyethylene tunnel type greenhouse. Renewable Energy 2003;28:683–97.
[4] Yuxian Xing, Xiufeng Wang, Tao Liu, Junling Li. Designing the optimum structure greenhouse with film plastic sunny side roof. J Shandong Agric Univ 1997;28(2):97–101.
[5] Barral Jorge R, Galimberti Pablo D, Barone Adrian, Lara Miguel A. Integrated thermal improvements for greenhouse cultivation in the central part of Argentina. Sol Energy 1999;67:111–8.
[6] Philp JR, Devries DA. Moisture movement in porous materials under temperature gradients. Trans Am Geophys Union 1957;38:222–32.
[7] Luikov AV. Heat and mass transfer in capillary porous-bodies. Oxford: Pergamon Press; 1966.
[8] Slattery JC. Two-phase flow through porous media. AICHE J 1970;16:345–54.
[9] Whitaker S. Simultaneous heat, mass and momentum transfer in porous media: a theory of drying. Advances in heat transfer. New York, NY: Academic Press; 1977.
[10] Milly PCD. A simulation analysis of thermal on evaporation from soil. Water Resour Res 1984;19:1087–98.

[11] Santamouris M, Argiriou A, Vallindras M. Design and operation of a low energy consumption solar agricultural greenhouse. Sol Energy 1994;52(5):371–8.
[12] Santamouris M, Balaras CA, Dascalaki E, Vallindras M. Passive solar agricultural greenhouse: a worldwide classification and evaluation of technologies and systems used for heating. Sol Energy 1994;53(5):411–26.
[13] Sallanbas H, Durceylan E, Yelboga K. Greenhouse heating with solar energy. In: Von Zabeltitz C, editor. FAO.
[14] Zhang Z, Liu W. Heat and moisture migration in the vertical porous bed. J Huazhong Univ Sci Tech 1993; 21:58–63.
[15] Liu W, Peng SW. Moisture evaporation and migration in tin porous packed bed influenced by ambient and operating conditions. Int J Energy Res 1997;21:41–53.
[16] Iacovides H, Raisee M. Computation of flow and heat transfer in two-dimensional rib-roughened passages using low-Reynolds-number turbulence models. Int J Num Methods Heat Fluid Flow 2001;11(2):138–55.
[17] Wei Chen, Wei Liu. Numerical and experimental analysis of convection heat transfer in passive solar heating room with greenhouse and heat storage. Sol Energy 2004;76(5):623–33.
[18] Wei Chen, Wei Liu. Numerical analysis of heat transfer in a composite wall solar collector system with a porous absorber. Appl Energy 2004;78(2):137–49.
[19] Patankar SV. Numerical heat transfer and fluid flow. New York, NY: Hemisphere Publishing Corp; 1980.
[20] Wen-Quan Tao. Numerical heat transfer. 2nd ed. Xian: Xian Jiaotong University Press; 2001.
[21] Qing-Fang Ma. Practical thermal physical property handbook. Beijing: The Chinese Agriculture Mechanics Press; 1986 pp. 701–10..